The Canadian Mineralogist
Vol. 40, pp. 1147-1159 (2002)

THE STRUCTURAL ROLE OF EXCESS Cu AND Pb IN GLADITE AND KRUPKAITE BASED ON NEW REFINEMENTS OF THEIR STRUCTURE

DAN TOPA[§], EMIL MAKOVICKY[¶] AND TONČI BALIĆ-ŽUNIĆ

Geological Institute, University of Copenhagen, Øster Voldgade 10, DK-1350 Copenhagen K, Denmark

ABSTRACT

Crystal structures of stoichiometric gladite (empirical formula $Cu_{1.32}Pb_{1.37}Bi_{6.65}S_{12.03}$) and krupkaite (empirical formula $Cu_{2.00}Pb_{2.03}Bi_{5.99}S_{12.04}$) from Felbertal, Austria, were refined to $R_1 = 0.045$ and 0.037, respectively, yielding improved positional parameters and interatomic distances. Structures of "oversubstituted" gladite with an excess of Pb + Cu substitution for Bi + tetrahedral vacancy (empirical formula $Cu_{1.55}Pb_{1.59}Bi_{6.43}S_{12.02}$, percentage of the aikinite end-member, $n_{aik} = 39$), of "undersubstituted" krupkaite ($Cu_{1.85}Pb_{1.92}Bi_{6.12}S_{12.06}$, $n_{aik} = 47$), and of "oversubstituted" krupkaite ($Cu_{2.32}Pb_{2.40}Bi_{5.64}S_{12.16}$, $n_{aik} = 59$) from the same locality, were refined to the R_1 values of 0.041, 0.051, and 0.052, respectively. Additional copper (occupancy 0.22) forms a broadly zig-zag pattern in each 1½ subcell of gladite. In "undersubstituted" krupkaite ($n_{aik} = 47$), the regular Cu position (Cu 1) was found to be slightly undersaturated. The "oversubstituted" krupkaite ($n_{aik} = 59$) contains additional Cu, located in the Cu 2 sites situated half-way between the fully occupied Cu 1 positions. Fixing their occupancy to 0.18, in agreement with EPMA data, and refining the adjacent large cation sites as two sites, with 0.18 Pb and 0.82 Bi, respectively, yielded the final model refined here. Interatomic distances and other characteristics of the polyhedra are used to evaluate the effects of cation substitution.

Keywords: gladite, krupkaite, oversubstitution, crystal structure, Felbertal, Austria.

SOMMAIRE

Nous avons affiné la structure cristalline de la gladite stoéchiométrique (formule empirique $Cu_{1.32}Pb_{1.37}Bi_{6.65}S_{12.03}$,) et de la krupkaïte (formule empirique $Cu_{2.00}Pb_{2.03}Bi_{5.99}S_{12.04}$) provenant de Felbertal, en Autriche, jusqu'à un résidu R_1 égal à 0.045 et 0.037, respectivement, ce qui a mené à des paramètres de position et des distances entre atomes améliorés. Les structures de la gladite "sursubstituée", contenant un excédent de Pb + Cu en substitution du Bi + lacune tétraédrique (formule empirique $Cu_{1.55}Pb_{1.59}Bi_{6.43}S_{12.02}$, pourcentage du pôle aikinite, $n_{aik} = 39$), de la krupkaïte "sous-substituée" ($Cu_{1.85}Pb_{1.92}Bi_{6.12}S_{12.06}$, $n_{aik} = 47$), et de la krupkaïte "sursubstituée" ($Cu_{2.32}Pb_{2.40}Bi_{5.64}S_{12.16}$, $n_{aik} = 59$), provenant du même endroit, ont été affinées jusqu'à un résidu R_1 de 0.041, 0.051, et 0.052, respectivement. Des atomes additionnels de cuivre (taux d'occupation à ce site égal à 0.22) sont répartis *grosso modo* en forme de zig-zag dans chaque 1½ sous-maille de gladite. Dans la krupkaïte "sous-substituée" ($n_{aik} = 47$), la position normale du Cu (Cu 1) serait légèrement sous-saturée. En revanche, la krupkaïte "sursaturée" ($n_{aik} = 59$) contient des atomes additionnels de Cu, situés aux sites Cu 2, à mi-chemin entre les sites Cu 1, remplis. En fixant leur taux d'occupation à 0.18, selon les données obtenues avec une microsonde électronique, et en affinant le site adjacent où logent les plus gros cations en supposant deux sites, avec 0.18 Pb et 0.82 Bi, respectivement, nous avons atteint le modèle final que nous décrivons ici. Les distances interatomiques et les autres caractéristiques des polyèdres servent à évaluer les effets de la substitution des cations.

(Traduit par la Rédaction)

Mots-clés: gladite, krupkaïte, sursubstitution, structure cristalline, Felbertal, Autriche.

§ *Present address*: Mineralogical Institute, University of Salzburg, Hellbrunnerstrasse 34/III, A-5020 Salzburg, Austria.
¶ *E-mail address*: emilm@geo.geol.ku.dk

Introduction

The bismuthinite–aikinite (Bi_2S_3–$CuPbBiS_3$) family of ordered substitution derivatives ranks among the best researched families of natural complex sulfides (sulfosalts). In the order of increasing substitution of Pb + Cu for Bi + vacancy, distinct structures have been established for bismuthinite (Kupčik & Veselá-Nováková 1970), pekoite, $CuPbBi_{11}S_{18}$ (Mumme & Watts 1976), gladite, $CuPbBi_5S_9$ (Syneček & Hybler 1974, Kohatsu & Wuensch 1976), krupkaite, $CuPbBi_3S_6$ (Syneček & Hybler 1974, Mumme 1975), lindströmite, $Cu_3Pb_3Bi_7S_{15}$ (Horiuchi & Wuensch 1977), hammarite, $Cu_2Pb_2Bi_4S_9$ (Horiuchi & Wuensch 1976) and aikinite, $CuPbBiS_3$ (Ohmasa & Nowacki 1970a, b, Kohatsu & Wuensch 1971).

Compositional ranges of individual members of this family were repeatedly investigated as well. A combination of electron-microprobe and single-crystal data was used in some of the above investigations, as well as by Harris & Chen (1976), Žák *et al.* (1975), Chen *et al.* (1978; friedrichite) and Welin (1966). Investigations combining electron-microprobe data with powder diffraction were performed by Borodayev *et al.* (1970), electron microdiffraction was added by Mozgova *et al.* (1990); HRTEM was used by Pring (1989, 1995), whereas the latest, most extensive set of electron-microprobe data, unaccompanied by diffraction experiments, comes from Ciobanu & Cook (2000).

The unusually rich spectrum of aikinite–bismuthinite derivatives from the deposit of Felbertal, Austria (Thalhammer *et al.* 1989), with a favorable mode of occurrence of single mineral grains or simple intergrowths in a quartz gangue, allowed us to perform single-crystal studies and crystal-structure determinations on a number of grains pre-analyzed with an electron microprobe. Compositional ranges of almost all derivatives mentioned above were tested, some space-group ambiguities resolved, and three new natural derivatives were found: a four-fold and a five-fold superstructure situated between gladite and krupkaite (Topa *et al.* 2000, Makovicky *et al.* 2001) and a new four-fold superstructure situated between krupkaite and aikinite (Balić-Žunić *et al.* 2002).

The present contribution concerns two minerals of the series, gladite (ideally $PbCuBi_5S_9$) and krupkaite (ideally $PbCuBi_3S_6$). Crystal-structure determinations on nearly ideal compositions have allowed us to further refine their structures. Structure determinations on both phases, oversubstituted (or undersubstituted) by Cu + Pb with respect to the ideal compositions, allow the direct establishment of the structural position of excess Cu (and Pb) and a discussion of the nature of this "oversubstitution" in more than hypothetical terms. Previous determinations of the structure were performed for both phases by Syneček & Hybler (1974; R = 0.18 and 0.25, respectively, for krupkaite and gladite), for gladite by Kohatsu & Wuensch (1976; R = 0.14), and for krupkaite by Mumme (1975, R = 0.097). Our results will be contrasted with those of Pring (1989), obtained by HRTEM, who offered an alternative insight into substitutional models for the aikinite–bismuthinite series.

Throughout this study, the practical way of describing the compositions of the phases studied, proposed by Makovicky & Makovicky (1978), will be adopted. All phases and structures will be treated as members of the composition series aikinite (x) – bismuthinite (100–x) or, in a short form, they will be characterized by n_{aik} corresponding to the percentage of the $CuPbBiS_3$ end-member in the Bi_2S_3–$CuPbBiS_3$ series. The value of n_{aik} will be indicated in parentheses after the mineral name. Ideal gladite, $CuPbBi_5S_9$, has n_{aik} = 33.33, whereas ideal krupkaite, $CuPbBiS_3$, has n_{aik} = 50.0.

Experimental

The crystals examined come from the orebodies K3 and K7 of the Felbertal tungsten ore deposit (Topa *et al.* 2002). Gladite (n_{aik} = 34), oversubstituted gladite (n_{aik} = 39), undersubstituted krupkaite (n_{aik} = 47), and krupkaite (n_{aik} = 50) come from a copper-undersaturated assemblage from level 4 (1038 m above sea level) of the orebody K3. This assemblage also yielded two other members of the bismuthinite–aikinite series, salzburgite (n_{aik} = 40) (Topa *et al.* 2000) and paarite (n_{aik} = 42) (Makovicky *et al.* 2001). Oversubstituted krupkaite occurs in the copper-saturated assemblage of the orebody K7 (level 6, 1100 m above sea level), in which emilite ($66 < n_{aik} < 68$) (Balić-Žunić *et al.* 2002), hammarite and lindströmite are present as well.

The chemical composition of the crystals was obtained by electron-microprobe analysis before their extraction from polished sections. We used a JEOL–8600 electron microprobe equipped with Link EXL software with on-line ZAF correction. Analytical conditions employed were 25 kV and 30 nA; synthetic and natural sulfide standards were used. The analytical results (wt.%) and the resulting empirical formulae are summarized in Table 1.

All crystals studied have an irregular shape and are 0.02–0.10 mm in diameter (Table 2). They were measured on a Bruker AXS four-circle diffractometer equipped with CCD 1000K area detector (6.25 cm × 6.25 cm active detection-area, 512 × 512 pixels) and a flat graphite monochromator using Mo$K\alpha$ radiation from a fine-focus sealed X-ray tube. Experimental and refinement data are summarized in Table 2. The SMART system of programs was used for unit-cell determination and data collection, SAINT+ for the calculation of integrated intensities, and SHELXTL for the structure solution and refinement (all Bruker AXS products). For the empirical absorption correction, based on reflection measurements at different azimuthal angles and measurements of equivalent reflections, program XPREP from SHELXTL package was used, and yielded merging R_{INT} factors (for equivalents) ranging from

0.051 to 0.088, compared to 0.10–0.21 before the absorption correction (Table 2). The systematic absences were carefully checked, and space groups *Pmcn* and $Pmc2_1$ were respectively chosen as consistent with structures of the bismuthinite–aikinite family. The structures were solved by direct methods, which suggested a solution revealing the positions of Bi and Pb atoms together with principal Cu sites and the S atoms. In subsequent refinements, the positions of the remaining Cu sites with lower occupancies were deduced from the difference-Fourier syntheses.

In the final refinements, anisotropic temperature-factors were used for all the atoms except for the partly occupied Cu positions and the split (Pb,Bi) position in krupkaite (n_{aik} = 59). The refinements were stopped when the maximum shift/e.s.d. for varied parameters dropped below 1. The results of the refinements are presented in Table 3, as well as in Figures 1–4, with interatomic distances in Table 4 (deposited). Structure factors may be obtained from the Depository of Unpublished Data, CISTI, National Research Council, Ottawa, Ontario K1A 0S2, Canada.

Description of the Structures

Principles of the structure

The crystal structures of minerals of the bismuthinite–aikinite series are ordered superstructures of the crystal structure of bismuthinite, Bi_2S_3. These superstructures are formed as a result of gradual, step-wise replacement of a half of the bismuth sites in the structure by lead. Parallel to this replacement is the filling of adjacent tetrahedrally coordinated sites by copper, resulting in the scheme Bi^{3+} + "tetrahedral vacancy" → Pb^{2+} + Cu^{+} (Figs. 1, 2).

TABLE 1. COMPOSITION OF THE GLADITE AND KRUPKAITE CRYSTALS STUDIED, AS DETERMINED BY ELECTRON-MICROPROBE ANALYSIS

wt.%	Points	Cu	Fe	Pb	Bi	Sb	S	Total
Gladite	5	3.84(3)	0.05(1)	13.4(1)	64.3(1)	0.0	17.88(4)	99.5(1)
Gladite	12	4.59(5)	0.00	15.3(1)	62.7(2)	0.0	17.98(3)	101.6(3)
Krupkaite	5	5.36(4)	0.00	18.1(1)	58.2(1)	0.07(1)	17.63(5)	99.6(2)
Krupkaite	4	5.82(5)	0.00	19.3(1)	57.3(2)	0.10(1)	17.78(8)	100.3(3)
Krupkaite	6	6.65(9)	0.00	22.4(3)	53.2(5)	0.00	17.60(6)	99.9(3)

apfu	Cu	Pb	Bi	S	n_{aik}	Δn_{aik}	eV
Gladite	1.32	1.37	6.65	12.03	33.7	0.6	-0.12
Gladite	1.55	1.59	6.43	12.02	39.2	0.5	-0.04
Krupkaite	1.85	1.92	6.12	12.06	47.1	0.9	-0.37
Krupkaite	2.00	2.03	5.99	12.04	50.3	0.4	-0.25
Krupkaite	2.32	2.40	5.64	12.16	59.0	1.0	-1.19

The formula is based on a sum of cations in a bismuthinite-like subcell.
n_{aik} is the percentage of the aikinite end-member in the solid solution Bi_2S_3–$CuPbBiS_3$ calculated as $n_{aik} = 12.5\ (x + y)$ for the empirical formula $Cu_xPb_yBi_{8-(x+y)/2}S_{12}$ ($x \approx y$) (Makovicky & Makovicky 1978). Δn_{aik} is equal to $|12.5\ (y - x)|$; eV is a charge-balance error per formula unit (*pfu*).

The crystal structure of bismuthinite and of its derivatives consists of tightly bonded ribbons Me_4S_6 that accommodate two distinct cation sites, the apical Bi site (denoted as Bi 1 in bismuthinite) and the central (inner) *Me* 2 site. It is the latter site where the gradual replacement of Bi 2 by Pb can proceed. Ribbons are arranged in a herring-bone pattern, the apical portions of one ribbon facing the central portion of the adjacent ribbon *via* the (empty) tetrahedral void.

Inside the ribbon, cations have a distorted square pyramidal coordination, which can be described in the case of Bi as MeS_{3+2}. Full coordination polyhedra of both Bi 1 and *Me* 2 sites have a coordination number (CN) equal to 7, *i.e.*, MeS_{3+2+2}. Both polyhedra are monocapped trigonal coordination prisms that involve sulfur atoms from adjacent ribbons. They are oriented at 90° and 0°, respectively, to the 4-Å-long *a* axis. These coordination prisms incorporate the lone-electron pairs of Bi and Pb in their prismatic portions. Thus the lone-electron pairs are all concentrated in the spaces between the ribbons, contributing to the good cleavage of these minerals.

In the structures examined, either unsubstituted "bismuthinite-like ribbons" Bi_4S_6, or half-substituted "krupkaite-like ribbons" $CuPbBi_3S_6$ are the principal components, and are combined in them, in an ordered fashion, in different proportions. Oversubstituted krupkaite will also contain a small percentage of "aikinite-like ribbons" with both *Me* 2 sites substituted by Pb, resulting in the ideal composition $Cu_2Pb_2Bi_2S_6$ for the ribbon.

The site notation adopted for oversubstituted phases (Figs. 1, 2) follows that used for stoichiometric phases; the additional cation sites are denoted as Cu 2 in both structures. Therefore, no separate figures with site labeling are introduced for unsubstituted gladite and krupkaite.

The stoichiometric phases

The crystal structure of *gladite* (n_{aik} = 33.7) refined to $R_1 = 0.045$ in space group *Pmcn*; it thus confirms that derived by Syneček & Hybler (1974) and Kohatsu & Wuensch (1976). It contains only one Cu and one Pb position (Fig. 3a), these being concentrated in four "krupkaite-like ribbons" $CuPbBi_3S_6$ (Ohmasa & Nowacki 1970a, Mumme *et al.* 1976) in the unit cell. Two additional "bismuthinite-like ribbons" Bi_4S_6 centered on $y = 0$, $z = 0$ and $y = 0.5$, $z = 0.5$, complete the picture. The Cu atoms are concentrated along two (010) planes, at $y = 0.25$ and 0.75, respectively, with Cu-free interspaces that are 1½ bismuthinite-like subcells wide. Any [010] row of *en échelon* Me_4S_6 ribbons has the sequence krupkaite–krupkaite–bismuthinite, with the

Pb-substituted part of the krupkaite-like ribbons oriented toward the bismuthinite-like ribbon.

The crystal structure of *krupkaite* (n_{aik} = 50.3) refined to R_1 = 0.037 in space group $Pmc2_1$; it thus agrees in principle with the results obtained by Syneček & Hybler (1974) and Mumme (1975). It again contains only one kind of Cu and Pb atoms, exclusively in krupkaite-like ribbons (Fig. 3b). The Cu atoms are concentrated along (010) planes at y = 0.5, a full 11 Å cell width apart, the site occupancy being equal to 1.0. The alternative Cu positions at y = 0 were found to be empty, contrary to the findings of Mumme (1975), who found 0.2 Cu in these and only 0.8 in the former sites.

The non-stoichiometric phases

The "oversubstituted" *gladite* (n_{aik} = 39.2) was refined to R_1 = 0.041 in the same space group as the stoichiometric compound, *Pmcn*. Atom positions differ insignificantly from those in the stoichiometric phase. Besides the fully occupied Cu 1 position, identical to that in the stoichiometric phase, a new partly occupied position, Cu 2, was found (Figs. 1, 4a). Its occupancy has been refined to 0.223, indicating the chemical formula $Cu_{4.89}Pb_{4.89}Bi_{19.11}S_{36}$, close to the empirical microprobe-established composition, $Cu_{4.65}Pb_{4.77}Bi_{19.29}S_{36.06}$ (the latter suggesting Cu 2 occupancy based on the n_{aik} value in Table 1, equal to 0.178). The correlation coefficient between the site occupancy of Cu 2 and its isotropic displacement factor (Table 3) is below 0.5. Cu 2 forms a broadly zig-zag pattern in every 1½ subcell interval situated between the (010) planes fully occupied by Cu 1. This distribution corresponds entirely to the distribution of Cu 4 and Cu 5 (site occupancy 0.1) in the same type of intervals in the structure of salzburgite $Cu_{1.6}Pb_{1.6}Bi_{6.4}S_{12}$ (Topa *et al.* 2000). In both cases, the "krupkaite-like" ribbons statistically acquire an "aikinite-like" character, whereas the "bismuthinite-like" ribbons remain unchanged.

The "undersubstituted" *krupkaite* (n_{aik} = 47.1) yielded only one Cu and one Pb position (Table 3). Our attempts to refine the occupancy of the slightly deficient Cu site showed that the correlation between the site occupancy and temperature factors (0.54) precludes significant results. With both variables free to refine, the occupancy refined to 1.00, whereas for the refinement

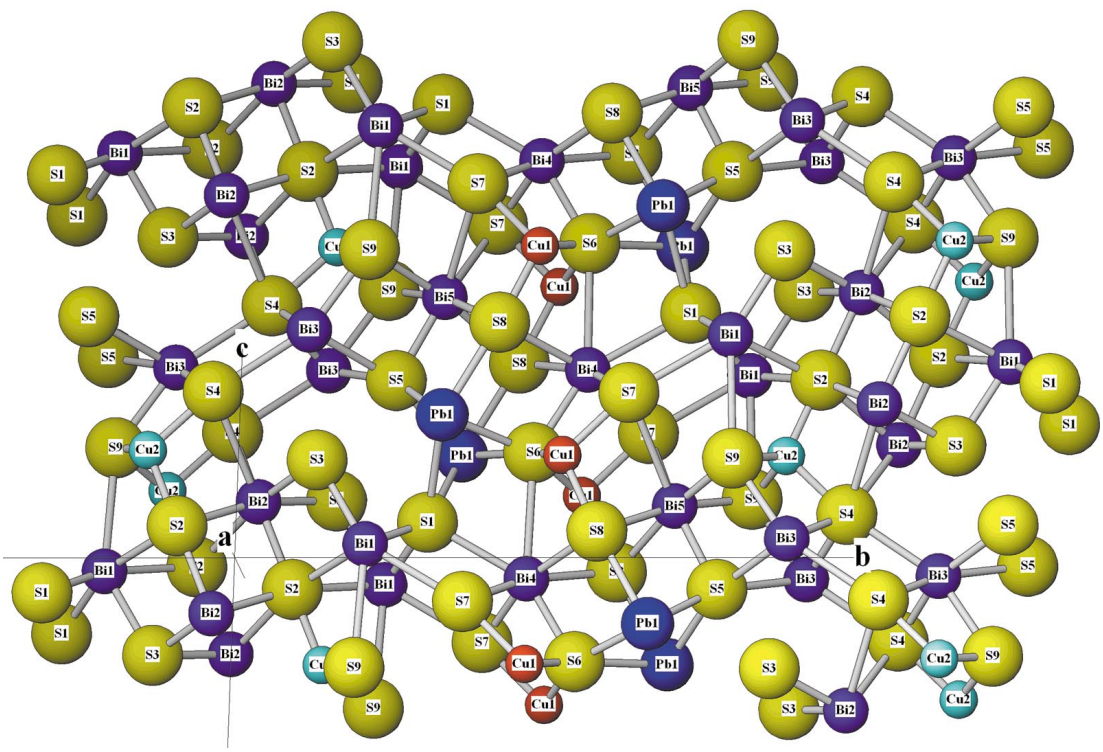

FIG. 1. A part of the crystal structure of oversubstituted gladite (n_{aik} = 39) with the atom coordinations and atom labels. The lengths and directions of the half-axes are indicated. Color code: fully occupied Cu positions: red, partially occupied positions (22.3% occupancy): turquoise.

of the anisotropic temperature-factor, the equivalent isotropic temperature-factor U_{eq} was 0.044 (R_1 = 0.051). When the occupancy was fixed to the microprobe-determined value of 0.940, the equivalent isotropic temperature-factor dropped for the anisotropic refinement to 0.0408. On the contrary, for an isotropic temperature-factor fixed to 0.042 (a compromise value between the above refinements), the occupancy of the Cu site refined to 0.975; this refinement is reported in Table 3. The R_1 value remains constant for all these variations within the bounds of $\Delta R_1 = 0.0001$.

Atom coordinates were practically identical in all the refinements attempted ($\Delta x_i \approx 0.0001$) and equal to those of krupkaite (n_{aik} = 50).

The "*oversubstituted krupkaite*" (n_{aik} = 59.0) lies at the upper end of the composition range of krupkaite, next to the composition of lindströmite (n_{aik} = 60) (Horiuchi & Wuensch 1977, Topa *et al.*, in prep.). It has two copper sites: Cu 1, which was refined as fully occupied, and Cu 2, a partly occupied site situated halfway between the (010) planes occupied by Cu 1 (Figs. 2, 4b). The Cu 2 site shows very high correlation (coefficient = 0.90) between the site occupancy and the temperature factor; a free refinement converges to an occupancy of about 0.073 with U_{iso} = 0.001, to be compared with U_{eq} = 0.042 for the fully occupied Cu 1 position. When the latter value is used and kept fixed for Cu 2, the refined occupancy is 0.123, yielding 2.246 Cu *apfu*; when the microprobe data are used to fix the occupancy of the Cu 2 site at 0.18 *apfu*, its U_{iso} refines as 0.0498. In the same refinement, the Bi 3 site was split into separate Bi and Pb positions, with occupancies fixed to 0.82 and 0.18, respectively. These positions were refined with free coordinates and isotropic displacement factors (Table 3, footnote). For all these cases, R_1 is equal to 0.052. As illustrated in Table 3, U_{eq} for Bi atoms lies at 0.035–0.036 except for Bi 3 (0.045), *i.e.,* for the site of partial Pb-for-Bi exchange connected with the partially occupied Cu 2 site. The atom coordinates are virtually identical for all these models, variations taking place on the fourth decimal place.

Coordination polyhedra

The precisely refined structures described in this study allow us to calculate improved data for the interatomic distances, bond angles and polyhedron characteristics for the cations involved (Tables 4–6). New

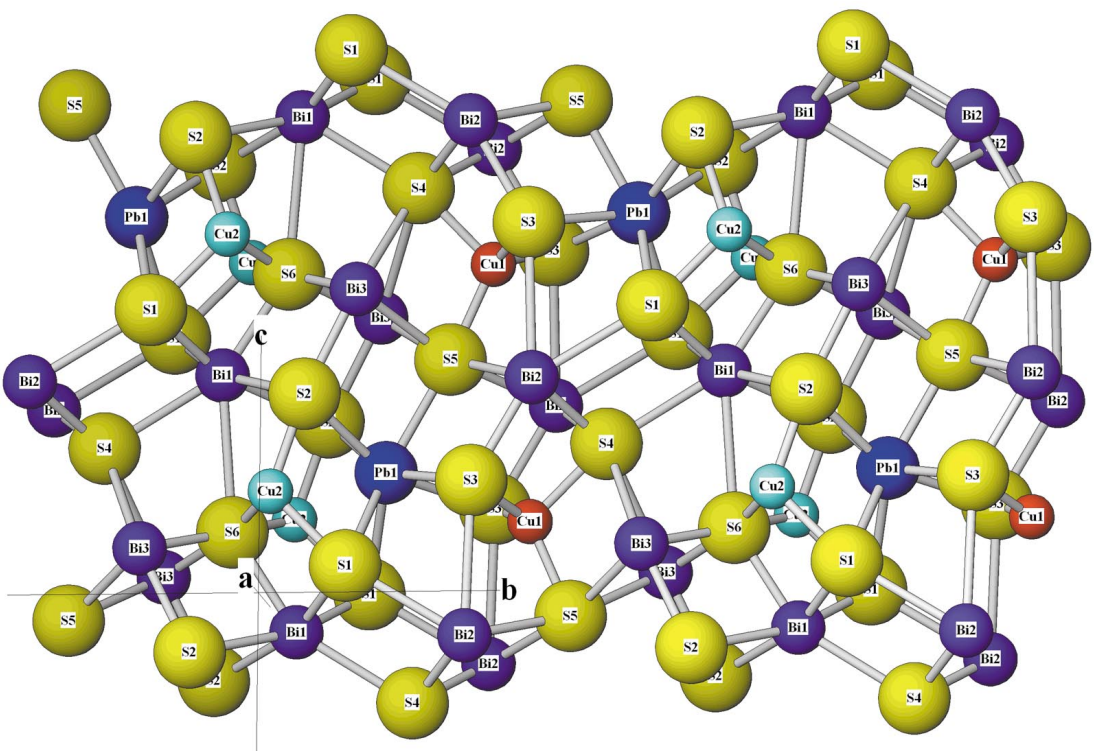

FIG. 2. A part of the crystal structure of oversubstituted krupkaite (n_{aik} = 59). Fully occupied Cu positions are indicated in red, partly occupied ones (12% occupancy) in turquoise.

TABLE 2. INFORMATION ABOUT THE GLADITE AND KRUPKAITE CRYSTALS SELECTED, DETAILS ABOUT THE COLLECTION OF DATA, AND THE REFINEMENT PROCEDURE

Sample label	bd33	bd39	bd47	bd50	bd59
Crystal data					
Structural formula	$Cu_{1.33}Pb_{1.33}Bi_{6.67}S_{12}$	$Cu_{1.63}Pb_{1.63}Bi_{6.37}S_{12}$	$Cu_{1.95}Pb_{1.95}Bi_{6.05}S_{12}$	$Cu_{2.00}Pb_{2.00}Bi_{6.00}S_{12}$	$Cu_{2.25}Pb_{2.25}Bi_{5.75}S_{12}$
Chemical form. wt	2138.69	2157.27	2172.65	2180.06	2202.29
Space group	*Pmcn*	*Pmcn*	$Pmc2_1$	$Pmc2_1$	$Pmc2_1$
a (Å)	4.0044(4)	4.0100(3)	4.0134(4)	4.0145(4)	4.0212(5)
b (Å)	33.575(3)	33.589(3)	11.208(1)	11.202(1)	11.232(1)
c (Å)	11.480(1)	11.502(1)	11.560(1)	11.560(1)	11.581(1)
V (Å)	1543.4(2)	1549.2(2)	520.0(1)	519.9(1)	523.1(1)
Z	3	3	1	1	1
D_x (Mg m^{-3})	6.903	6.925	6.938	6.963	6.991
No. of reflexions for cell param.	3516	4134	2790	2177	2255
μ (mm^{-1})	70.198	70.089	69.799	69.889	69.685
F(000)	2680	2700	909	912	922
Crystal size (mm)	0.08 × 0.05 × 0.04	0.08 × 0.04 × 0.02	0.08 × 0.054 × 0.036	0.10 × 0.07 × 0.03	0.08 × 0.05 × 0.03
Data collection					
Detector–sample distance (mm)	60	60	40	60	60
Number of frames	2080	2080	2600	2080	2080
Width of frames (°)	0.25	0.25	0.20	0.25	0.25
Measurement time (s)/frame	60	60	45	30	60
Min. transmission	0.00123	0.00339	0.00165	0.00316	0.00138
Max. transmission	0.01335	0.01892	0.02022	0.02073	0.01651
No. of measured reflections	8856	8954	5299	3075	3140
No. of unique refl.	1745	1800	1760	1176	1154
No. of observed refl. ($I > 2\sigma_I$)	1444	1566	1625	1133	1123
R_{int}	0.0596	0.0548	0.0767	0.0652	0.0783
R(σ)	0.0330	0.0308	0.0589	0.0517	0.0512
θ_{min} (°)	3.60	3.51	4.04	3.64	3.52
θ_{max} (°)	26.86	26.92	30.49	26.77	26.78
Range of *h, k, l*	$-4 \le h \le 3$	$-4 \le h \le 5$	$-5 \le h \le 5$	$-4 \le h \le 5$	$-4 \le h \le 5$
	$-40 \le k \le 41$	$-40 \le k \le 41$	$-15 \le k \le 16$	$-13 \le k \le 13$	$-13 \le k \le 12$
	$-13 \le l \le 14$	$-14 \le l \le 13$	$-16 \le l \le 16$	$-14 \le l \le 14$	$-14 \le l \le 14$
Coverage (to θ max.)	91.8%	94%	99.3%	95.8%	95.4%
Refinement (of F^2 against all reflections)					
R ($Fo>4\sigma_{Fo}$)	0.0454	0.0405	0.0508	0.0373	0.0519**
R_{all}	0.0530	0.0464	0.0535	0.0387	0.0525
wR ($Fo>4\sigma_{Fo}$)	0.1091	0.1029	0.1185	0.0925	1386
wR_{all}	0.1135	0.1064	0.1197	0.0933	1392
Goof	0.992	1.111	1.058	1.084	1.123
No. of refl. used	1745	1800	1760	1176	1154
No. of parameters	98	101	64	67	70
No. of restraints	0	0	1	1	1
*Weight. scheme factors: a, b	0.0821 0.0	0.0678 2.0139	0.0801 0.0	0.0593 0.0	0.0992 2.3094
$(\Delta\rho)_{max}$ (e $Å^{-3}$)	2.70	4.03	4.17	2.15	3.61
$(\Delta\rho)_{min}$ (e $Å^{-3}$)	–2.73	–4.21	–2.15	–3.02	–3.27
scale factor	0.03560	0.03245	0.06787	0.06822	0.07825
Extinction coeff.	0.000025	0.00003(5)	–	–	–

* $w = 1/[\sigma^2_{Fo}{}^2 + (a \cdot P)^2 + bP]$, where $P = (Fo^2 + 2Fc^2)/3$. ** for a refinement with unsplit (Bi,Pb)3 positions. bd: bismuthinite derivative.

structure refinements for Bi_2S_3 (Lundgaard *et al.*, in prep.) and $CuPbBiS_3$ (Topa *et al.*, in prep.) will be used for comparison. The following site-notation is used (Figs. 1, 2): In the refined structure of gladite, Bi 1 is the terminal and Bi 2 the central coordination-polyhedron of bismuth in the "bismuthinite-like" ribbon. Bi 3 and Bi 4 are the terminal polyhedra, whereas Bi 5 and Pb 1 are the "central" polyhedra of "krupkaite-like" ribbons. Bi 3 and Bi 5 are on one side of the ribbon, whereas Bi 4 and the Pb site are on the other side of the ribbon. Cu 1 is associated with Pb 1, whereas Cu 2 in gladite (n_{aik} = 39) is linked to the mixed (Bi,Pb)5 position (Fig. 1). In all the refined structures of krupkaite, Bi 1 and Bi 2 denote terminal coordination-polyhedra of bismuth, whereas Pb 1 and Bi 3 (with respect to the split positions Bi 3 and Pb 2) are the central polyhedra of the Me_4S_6 ribbons. Bi 2 is marginal to Pb 1 and adjacent to the filled Cu 1 tetrahedron. Bi 1 and Bi 3 represent the "bismuth side" of the krupkaite-like ribbon (Fig. 2).

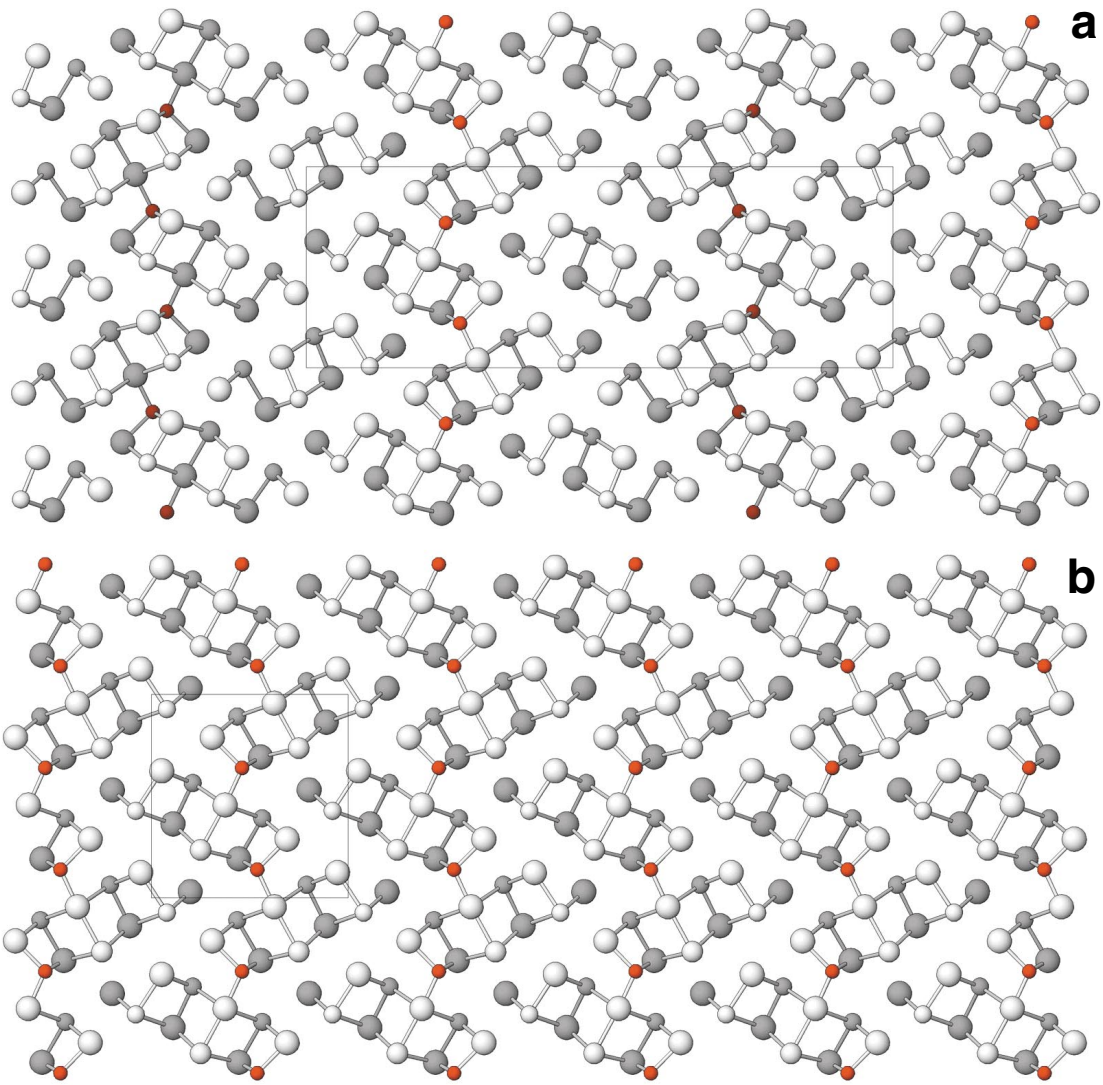

FIG. 3. (a) The crystal structure of stoichiometric gladite, with 33% of the aikinite end-member. (b) The crystal structure of stoichiometric krupkaite (n_{aik} = 50). In the order of increasing size, circles represent Cu (fully occupied positions, in red), bismuth, lead and sulfur. Shaded and void circles indicate two levels in *x*, approximately 2 Å apart. Projections along [100], *b* axis horizontal, *c* vertical.

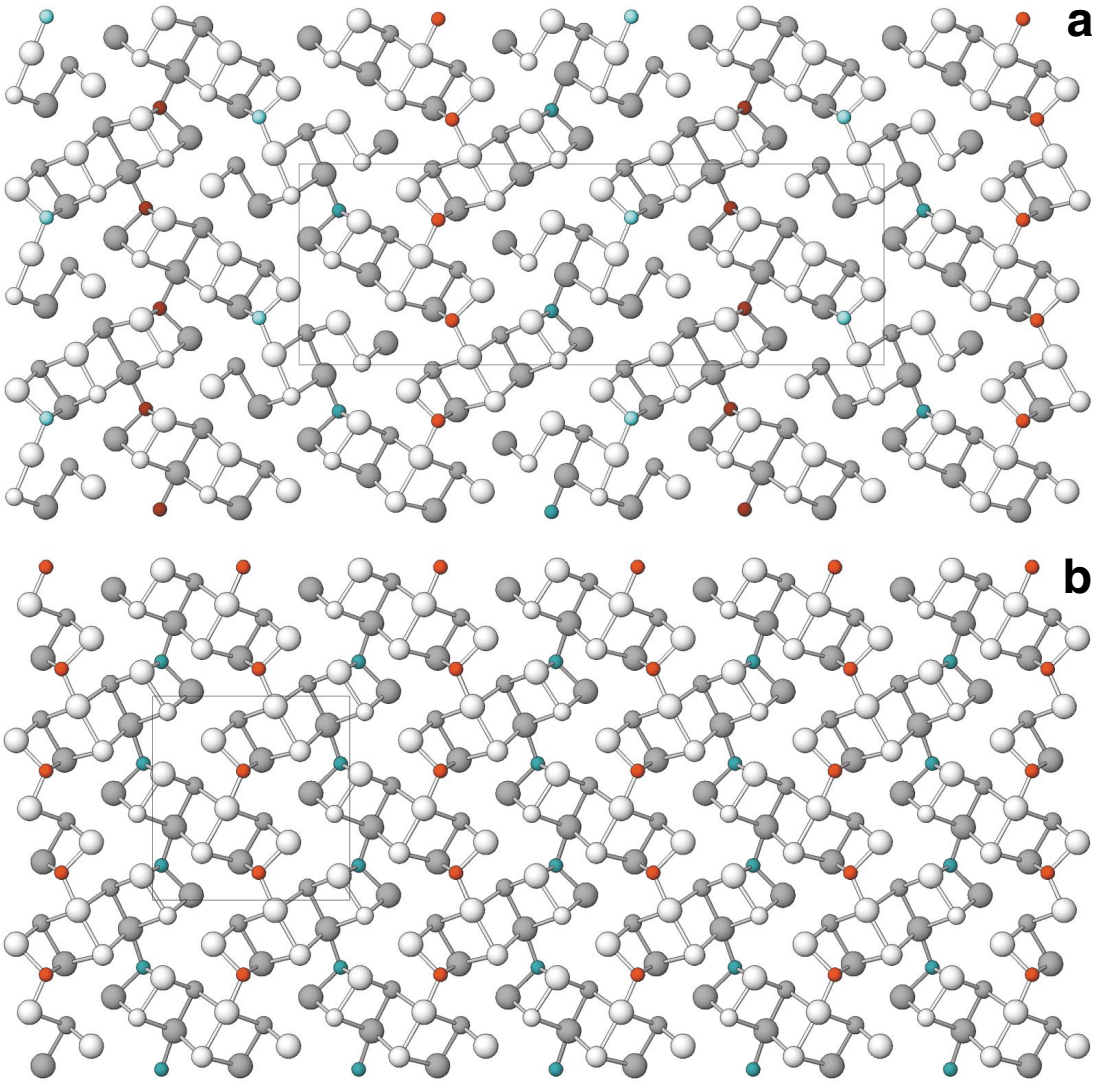

FIG. 4. (a) The crystal structure of oversubstituted gladite (n_{aik} = 39). (b) The crystal structure of oversubstituted krupkaite (n_{aik} = 59). The fully occupied Cu positions are indicated in red, the partly occupied ones (22% in gladite, 12% in krupkaite) in blue.

There is a significant general increase in the volumes V_P of the Bi polyhedra and those of their circumscribed spheres (V_s) with the increase in the overall Cu-and-Pb-for-vacancy-and-Bi substitution, from bismuthinite (Bi 1: V_P and V_s respectively equal to 36.33 Å^3 and 106.93 Å^3, Bi 2: 36.10/109.10 Å^3) toward the structures studied. A similar increase can also be observed in comparing the present Pb sites with the position of lead in aikinite (V_P/V_s = 40.15 Å^3/120.84 Å^3). There are no systematic differences between the two structures investigated, gladite and krupkaite, in comparisons of the corresponding terminal Bi positions, except for the observable influence of the adjacent Pb (Tables 5, 6). The differences between these two structures are concentrated in the central Bi positions.

In gladite, the Bi 1 and Bi 2 sites are in the "bismuthinite-like" ribbon. Their distortion characteristics are similar to those of Bi sites in Bi_2S_3, but the

TABLE 3. POSITIONAL AND DISPLACEMENT PARAMETERS FOR THE GLADITE AND KRUPKAITE STRUCTURES REFINED

Atom	occ.	*x*	*y*	*z*	U_{eq}	U_{11}	U_{22}	U_{33}	U_{23}
				Gladite (n_{aik} = 33)					
Bi1		0.25	0.39201(2)	0.50696(7)	0.0421(2)	0.0388(4)	0.0442(4)	0.0432(4)	0.0040(3)
Bi2		0.75	0.48687(2)	0.65683(7)	0.0434(2)	0.0434(4)	0.0456(5)	0.0412(4)	-0.0007(3)
Bi3		0.25	0.05623(2)	0.52112(7)	0.0415(2)	0.0388(4)	0.0412(4)	0.0444(4)	0.0030(3)
Bi4		0.75	0.27078(2)	0.47365(7)	0.0424(2)	0.0399(4)	0.0470(5)	0.0404(4)	0.0021(3)
Bi5		0.75	0.15429(2)	0.64885(7)	0.0439(2)	0.0438(4)	0.0447(5)	0.0432(4)	-0.0031(3)
Pb		0.25	0.16511(3)	0.31833(7)	0.0485(3)	0.0477(5)	0.0512(5)	0.0468(5)	0.0049(3)
Cu		0.25	0.23783(8)	0.7205(2)	0.0490(6)	0.048(1)	0.055(1)	0.043(1)	-0.002(1)
S1		0.75	0.3516(1)	0.6086(4)	0.040(1)	0.043(2)	0.038(2)	0.039(2)	0.004(2)
S2		0.75	0.4581(1)	0.4482(4)	0.039(1)	0.039(2)	0.039(2)	0.039(2)	0.000(2)
S3		0.25	0.4333(1)	0.7088(4)	0.037(1)	0.037(2)	0.035(2)	0.039(2)	-0.001(2)
S4		0.75	0.0178(1)	0.6279(4)	0.041(1)	0.040(2)	0.040(2)	0.042(3)	0.002(2)
S5		0.75	0.1190(1)	0.4484(4)	0.039(1)	0.038(2)	0.038(2)	0.040(2)	0.002(2)
S6		0.75	0.2306(1)	0.2743(4)	0.039(1)	0.039(2)	0.038(2)	0.038(2)	0.000(2)
S7		0.25	0.3132(1)	0.3714(4)	0.040(1)	0.043(2)	0.037(2)	0.041(2)	-0.001(2)
S8		0.25	0.2081(1)	0.5379(4)	0.040(1)	0.041(2)	0.044(2)	0.037(2)	0.000(2)
S9		0.25	0.1023(1)	0.7130(4)	0.037(1)	0.037(2)	0.037(2)	0.039(2)	-0.001(2)
				Gladite (n_{aik} = 39)					
Bi1		0.25	0.39243(3)	0.50808(7)	0.0363(3)	0.0339(5)	0.0374(5)	0.0377(5)	0.0044(3)
Bi2		0.75	0.48697(3)	0.65794(8)	0.0407(3)	0.0379(5)	0.0429(5)	0.0414(5)	0.0032(4)
Bi3		0.25	0.05679(2)	0.52041(7)	0.0358(3)	0.0338(5)	0.0343(5)	0.0392(5)	0.0022(3)
Bi4		0.75	0.27130(3)	0.47335(7)	0.0360(3)	0.0343(5)	0.0394(5)	0.0343(5)	0.0020(3)
Bi5		0.75	0.15535(3)	0.64725(8)	0.0397(3)	0.0406(5)	0.0398(5)	0.0386(5)	-0.0035(3)
Pb1		0.25	0.16514(3)	0.31690(8)	0.0422(3)	0.0431(5)	0.0431(5)	0.0405(5)	0.0040(4)
Cu1		0.25	0.23800(9)	0.7207(2)	0.0419(7)	0.042(1)	0.046(2)	0.037(1)	-0.004(1)
Cu2	0.223(7)	0.75	0.4318(3)	0.2672(8)	0.042*				
S1		0.75	0.3517(2)	0.6088(5)	0.033(1)	0.036(3)	0.032(3)	0.032(2)	0.001(2)
S2		0.75	0.4574(2)	0.4484(5)	0.033(1)	0.035(2)	0.031(3)	0.033(2)	0.000(2)
S3		0.25	0.4332(2)	0.7091(4)	0.031(1)	0.034(3)	0.027(2)	0.032(2)	0.001(2)
S4		0.75	0.0180(2)	0.6268(4)	0.033(1)	0.035(3)	0.032(3)	0.032(3)	0.001(2)
S5		0.75	0.1192(2)	0.4480(5)	0.032(1)	0.035(3)	0.029(3)	0.032(2)	0.001(2)
S6		0.75	0.2307(2)	0.2753(5)	0.032(1)	0.033(2)	0.028(2)	0.034(3)	0.000(2)
S7		0.25	0.3132(2)	0.3702(4)	0.034(1)	0.038(3)	0.031(3)	0.032(2)	0.000(2)
S8		0.25	0.2082(2)	0.5385(5)	0.035(1)	0.038(3)	0.036(3)	0.031(2)	0.000(2)
S9		0.25	0.1023(2)	0.7126(4)	0.031(1)	0.035(2)	0.027(2)	0.032(3)	-0.001(2)

volumes are distinctly larger. Analysis of bond lengths shows that the short and intermediate Bi–S distances are broadly similar, whereas the longest Bi–S distances in the bismuthinite-like ribbon of gladite are longer than the corresponding distances in bismuthinite: 3.07 Å *versus* 3.04 Å for Bi 1 and 2 × 3.345 Å *versus* 2 × 3.323 Å for Bi 2. The increase in unit-cell parameters thus takes place primarily in the inter-ribbon spaces.

The terminal bismuth sites (Bi 4 in gladite and Bi 2 in krupkaite) that are attached to the central Pb 1 polyhedron have sphere and polyhedron volumes slightly larger than those attached to central Bi (Tables 5, 6). The central Bi atoms (Bi 5 in gladite and Bi 3 in krupkaite) in the "krupkaite-like" ribbons have larger volumes, eccentricities and volume distortions and lower sphericities than those in "bismuthinite-like" ribbons of gladite (Bi 2 in Table 5) or Bi_2S_3 (Table 6). These differences seem to be caused by a "sandwiching" between the large Pb 1 polyhedron on the one side and the Cu 1 tetrahedron on the other (Figs. 3a, b). A comparison of interatomic distances (Bi 2 in gladite: 2.582, 2 × 2.757, 2 × 2.979 and 2 × 3.345 Å *versus* Bi 5 in gladite: 2.588, 2 × 2.756, 2 × 2.983 and 2 × 3.424 Å) shows that the elongation of the lone-electron-pair-containing prismatic part of the Bi coordination polyhedron bears the bulk of these adjustments.

All the characteristics of the Pb 1 positions for krupkaite (n_{aik} = 47) and krupkaite (n_{aik} = 50) are virtually identical, although all the deviations in the $Pb_{94}Bi_6$ position in the former point in the right direction (*e.g.,* the polyhedron has a smaller volume and higher averaged eccentricity than the pure Pb position, Table 6). In krupkaite (n_{aik} = 59), the polyhedron and circumscribed-sphere volumes for this position noticeably increase, together with those of the other polyhedra (Bi 1 and Cu 1) that are influenced indirectly by cation exchange (Table 6). This increase is in agreement with the observed increase in the unit-cell volume, reflecting

TABLE 3 (cont'd). POSITIONAL AND DISPLACEMENT PARAMETERS FOR THE GLADITE AND KRUPKAITE STRUCTURES REFINED

Atom	occ.	*x*	*y*	*z*	U_{eq}	U_{11}	U_{22}	U_{33}	U_{23}
				Krupkaite (n_{aik} = 47)					
Bi1		0	0.92144(8)	0.42290(7)	0.0334(2)	0.0320(5)	0.0323(4)	0.0360(4)	0.0042(3)
Bi2		0.5	0.56408(8)	0.38615(8)	0.0344(2)	0.0341(5)	0.0362(4)	0.0330(4)	0.0023(3)
Bi3		0.5	0.21067(9)	0.55937(7)	0.0367(2)	0.0380(5)	0.0357(5)	0.0365(4)	-0.0032(3)
Pb1		0.0	0.2513(1)	0.23076(9)	0.0417(3)	0.0420(6)	0.0427(5)	0.0405(4)	0.0068(4)
Cu1	0.98(1)	0	0.4611(4)	0.6332(3)	0.042*				
S1		0.5	0.8029(5)	0.5255(5)	0.031(1)	0.034(3)	0.027(2)	0.032(2)	0.000(2)
S2		0.5	0.1106(6)	0.3577(5)	0.032(1)	0.034(3)	0.032(3)	0.030(2)	0.000(2)
S3		0.5	0.4446(5)	0.1885(5)	0.032(1)	0.033(3)	0.030(3)	0.034(3)	-0.002(2)
S4		0.0	0.6904(5)	0.2822(5)	0.033(1)	0.042(3)	0.025(2)	0.032(2)	-0.004(2)
S5		0.0	0.3758(5)	0.4510(4)	0.030(1)	0.034(3)	0.028(3)	0.028(3)	-0.002(2)
S6		0.0	0.0531(5)	0.6201(5)	0.030(1)	0.033(3)	0.026(3)	0.031(2)	0.000(2)
				Krupkaite (n_{aik} = 50)					
Bi1		0	0.92106(9)	0.42767(8)	0.0323(3)	0.0310(5)	0.0330(5)	0.0328(6)	-0.0038(4)
Bi2		0.5	0.56344(9)	0.39079(9)	0.0330(3)	0.0315(5)	0.0379(5)	0.0295(5)	-0.0015(4)
Bi3		0.5	0.21048(9)	0.56429(8)	0.0352(3)	0.0347(5)	0.0377(5)	0.0330(5)	0.0038(4)
Pb1		0.0	0.2507(1)	0.2357(1)	0.0381(3)	0.0394(6)	0.0399(5)	0.0351(6)	0.0033(4)
Cu1		0.0	0.4612(3)	0.6386(3)	0.0390(8)	0.037(2)	0.048(2)	0.032(2)	0.003(2)
S1		0.5	0.8021(6)	0.5304(6)	0.031(1)	0.035(3)	0.029(3)	0.030(3)	-0.005(2)
S2		0.5	0.1104(6)	0.3629(6)	0.030(1)	0.030(3)	0.033(3)	0.027(3)	-0.004(2)
S3		0.5	0.4447(6)	0.1920(6)	0.033(1)	0.041(4)	0.034(3)	0.024(3)	0.004(3)
S4		0.0	0.6901(5)	0.2882(6)	0.029(1)	0.033(3)	0.028(3)	0.025(3)	0.002(3)
S5		0.0	0.3751(6)	0.4563(5)	0.032(1)	0.034(3)	0.036(3)	0.026(4)	0.002(3)
S6		0.0	0.0531(6)	0.6241(6)	0.028(1)	0.025(3)	0.031(3)	0.029(3)	0.001(3)
				Krupkaite (n_{aik} = 59)					
Bi1		0	0.9232(1)	0.4225(1)	0.0352(4)	0.0320(6)	0.0354(7)	0.0382(7)	0.0037(5)
Bi2		0.5	0.5641(1)	0.3857(1)	0.0359(4)	0.0328(7)	0.0389(7)	0.0360(6)	0.0007(5)
Bi3*		0.5	0.2134(1)	0.5602(1)	0.0452(4)	0.0384(7)	0.0509(9)	0.0462(7)	0.0018(7)
[Bi*	0.82	0.5	0.2105(3)	0.5585(2)	0.0402(8)]				
[Pb*	0.18	0.5	0.233(1)	0.572(1)	0.052(5)]				
Pb1		0.0	0.2516(1)	0.2307(1)	0.0418(4)	0.0404(8)	0.0408(7)	0.0441(7)	0.0051(6)
Cu1		0.0	0.4606(5)	0.6334(4)	0.042(1)	0.038(2)	0.050(3)	0.038(2)	0.000(2)
Cu2	0.12(1)	0.5	0.046(4)	0.169(4)	0.042**				
S1		0.5	0.8033(8)	0.5235(8)	0.033(2)	0.038(4)	0.026(4)	0.035(3)	0.004(3)
S2		0.5	0.1113(8)	0.3578(7)	0.034(2)	0.034(4)	0.032(4)	0.036(4)	0.002(3)
S3		0.5	0.4456(7)	0.1867(7)	0.031(2)	0.029(4)	0.027(4)	0.035(4)	0.001(3)
S4		0.0	0.6902(8)	0.2828(8)	0.034(2)	0.032(4)	0.030(4)	0.039(4)	0.001(4)
S5		0.0	0.3774(8)	0.4493(7)	0.037(2)	0.035(4)	0.036(5)	0.040(5)	-0.006(4)
S6		0.0	0.0532(8)	0.6178(8)	0.033(2)	0.031(4)	0.034(4)	0.034(4)	-0.001(3)

Note: The percentage of the aikinite end-member in the member of the bismuthinite–aikinite solid-solution series is indicated by n_{aik}. Full site occupancies where not indicated otherwise. * Oversubstituted krupkaite was also refined with the Bi3 position split into 0.82 Bi3 and 0.18 Pb2, respectively, giving the positional parameters and isotropic displacement factors indicated in square brackets. ** Fixed, equal to that of Cu1.

"oversubstitution". Both measures of volume for the terminal Bi 2 polyhedron remain constant in this exchange. In gladite, the presence of the partly occupied Cu 2 position seems to provoke more pronounced changes in the bond lengths and polyhedron volume (Table 5) of the Bi 2 position of the adjacent bismuthinite-like chain [2.607, 2 × 2.762, 2 × 3.002 and 2 × 3.352 Å] (to be compared with the values for gladite, n_{aik} = 33, as given above) than in the corresponding characteristics of the Bi 5 position in the krupkaite-like chains, to which Cu 2 is attached (2.593, 2 × 2.786, 2 × 2.956 and 2 × 3.423 Å, *versus* the values given above). This observation opens up a possibility of accommodating additional Pb in the central positions of the bismuthinite-like ribbons instead of in such portions of the krupkaite-like ribbons adjacent to Cu 2. This alternative deserves further investigation by appropriate diffraction methods.

The mixed "Bi3" position in krupkaite (n_{aik} = 59) shows clearly an augmented volume of polyhedron and

TABLE 5. POLYHEDRON CHARACTERISTICS FOR THE GLADITE STRUCTURES REFINED AND BISMUTHINITE

Atom	CN	Sphere radius	Sphere volume	Polyhedron volume	Volume distortion(1)	Eccentricity(2)	Sphericity(3)
$Bi1_{33}$	7	2.954	108.01	36.83	0.0989	0.3632	0.9677
$Bi1_{39}$	7	2.954	108.01	36.81	0.0995	0.3696	0.9604
$Bi2_{33}$	7	2.974	110.19	36.48	0.1252	0.4163	0.9611
$Bi2_{39}$	7	2.987	111.67	37.02	0.124	0.4111	0.9593
$Bi3_{33}$	7	2.956	108.23	36.6	0.1063	0.4199	0.8963
$Bi3_{39}$	7	2.958	108.37	36.67	0.1059	0.4166	0.8988
$Bi4_{33}$	7	2.957	108.32	37	0.097	0.377	0.9504
$Bi4_{39}$	7	2.963	109.02	37.18	0.0986	0.3847	0.9503
$Bi5_{33}$	7	3	113.05	37.25	0.1292	0.4483	0.9374
$Bi5_{39}$	7	3	113.07	37.29	0.1285	0.4367	0.9379
$Pb1_{33}$	7	3.031	116.69	38.42	0.1299	0.1642	0.977
$Pb1_{39}$	7	3.035	117.05	38.55	0.1297	0.1489	0.9735
$Cu1_{33}$	4	2.357	54.82	6.56	0.0239	0.0988	1
$Cu1_{39}$	4	2.356	54.79	6.54	0.0256	0.0929	1
$Cu2_{39}$	4	2.343	53.86	6.45	0.022	0.1195	1
Bi1	7	2.944	106.93	36.33	0.1022	0.3749	0.9625
Bi2	7	2.964	109.1	36.1	0.1255	0.409	0.9573
□tet	4	2.319	52.23	6.26	0.0219	–	1

Subscripts indicate the phases involved: gladite (n_{aik} = 33) and oversubstituted gladite (n_{aik} = 39). Bi 1 and Bi 2 are, respectively, the terminal and the central Bi positions in a ribbon of a newly refined structure of synthetic bismuthinite (in prep.). and □tet is the empty tetrahedral position in this structure. Sphere radius is expressed in Å, whereas sphere volume and polyhedron volume are expressed in Å^3. The centroid parameters (1) to (3) are explained in a footnote to Table 6.

sphere in this "oversubstituted" structure (Table 6), whereas other characteristics for the mixed polyhedron do not differ substantially from those of a pure Bi site (only the eccentricity drops marginally). After splitting, the independent Bi 3 site (occupancy 0.82) is highly eccentric, whereas the associated Pb 2 site has a significantly decreased eccentricity (Table 3). We were not able to model similar splitting for the mixed Bi site(s) in gladite (n_{aik} = 39).

A comparison of *Me*–S distances (Table 4, deposited) shows virtually no change between the Pb 1 position in krupkaite (n_{aik} = 59) and that in krupkaite (n_{aik} = 50): 2.900(10), 2 × 2.947(7), 2 × 3.012(7) and 2 × 3.189(7) Å in the former against 2.906(6), 2 × 2.943(5), 2 × 3.001(5) and 2 × 3.164(5) Å in the latter. The partly occupied Pb 2 position in n_{aik} = 59, associated with the Bi 3 position, has significantly shorter *Me*–S distances: 2.84(1), 2 × 2.90(1), 2 × 2.95(1) and a longer pair 2 × 3.28(2); this is caused by the *averaged character* of the surrounding sulfur positions. The asymmetry of interatomic distances for the Bi 3 position is augmented, apparently due to the enlargement of the (average) coordination polyhedron by insertion of substitutional Pb.

The fully occupied Cu 1 sites in krupkaite have a slightly eccentric tetrahedral coordination typical of the bismuthinite–aikinite derivatives. Their eccentricity (Table 6) is comparable with that for Cu 1 in aikinite (0.080, our data) and slightly lower than the values for fully occupied Cu sites in salzburgite, $Cu_{1.6}Pb_{1.6}Bi_{6.4}S_{12}$ (Topa *et al.* 2000) and in both gladite samples studied (Table 5). The polyhedron characteristics for the partly occupied Cu 2 sites (Figs. 4a, b, Tables 5, 6) resemble closely those of the full tetrahedrally coordinated sites. The differences observed can be ascribed to the results of averaging of S positions over the empty and filled tetrahedra around the partly occupied copper sites.

Modular aspects

Pring (1989) studied two variants of oversubstituted krupkaite, $Cu_{1.03}Pb_{1.03}Bi_{2.97}S_6$ and $Cu_{1.1}Pb_{1.1}Bi_{2.9}S_6$, as well as one sample of "ideal" krupkaite, $CuPbBi_3S_6$, by means of electron diffraction and HRTEM. He indicated the presence of faint disorder-induced streaks parallel

TABLE 6. POLYHEDRON CHARACTERISTICS FOR THE KRUPKAITE STRUCTURES REFINED

Atom	CN	Sphere radius	Sphere volume	Polyhedron volume	Volume distortion(1)	Eccentricity(2)	Sphericity(3)
$Bi1_{47}$	7	2.955	108.13	36.75	0.102	0.3907	0.9213
$Bi1_{50}$	7	2.956	108.2	36.78	0.1017	0.3937	0.9201
$Bi1_{59u}$	7	2.96	108.67	36.94	0.1018	0.4046	0.9213
$Bi1_{59s}$	7	2.96	108.68	36.93	0.102	0.4055	0.9208
$Bi2_{47}$	7	2.969	109.61	37.32	0.1004	0.3875	0.9451
$Bi2_{50}$	7	2.966	109.28	37.26	0.0989	0.3835	0.9464
$Bi2_{59u}$	7	2.967	109.36	37.26	0.0996	0.3816	0.9418
$Bi2_{59s}$	7	2.967	109.41	37.27	0.0997	0.3811	0.9426
$Bi3_{47}$	7	3.014	114.68	37.87	0.1273	0.4556	0.941
$Bi3_{50}$	7	3.015	114.78	37.85	0.1286	0.4613	0.9377
$Bi3_{59u}$	7	3.026	116.11	38.29	0.1285	0.4423	0.9449
$Bi3_{59s}$	7	3.026	116.07	38.28	0.1285	0.4666	0.9439
$Pb1_{47}$	7	3.023	115.69	38.22	0.1269	0.1562	0.975
$Pb1_{50}$	7	3.024	115.81	38.26	0.127	0.1536	0.9766
$Pb1_{59u}$	7	3.035	117.11	38.68	0.1272	0.1696	0.9761
$Pb1_{59s}$	7	3.035	117.1	38.71	0.1265	0.1691	0.9767
$Pb2_{59s}$		3.026	116.07	38.28	0.1285	0.2581	0.9439
$Cu1_{47}$		2.355	54.71	6.52	0.0276	0.0827	1
$Cu1_{50}$		2.354	54.61	6.51	0.0264	0.0853	1
$Cu1_{59u}$		2.358	54.92	6.55	0.0272	0.0788	1
$Cu1_{59s}$		2.357	54.82	6.54	0.027	0.0839	1
$Cu2_{59u}$		2.358	54.91	6.58	0.0217	0.0651	1
$Cu2_{59s}$		2.357	54.84	6.57	0.0219	0.0824	1

Notes: Subscripts indicate the phases involved: undersubstituted krupkaite (n_{aik} = 47), stoichiometric krupkaite (n_{aik} = 50), and oversubstituted krupkaite (n_{aik} = 59). The centroid parameters used defined in Balić-Žunić & Makovicky (1996) and Makovicky & Balić-Žunić (1998). The volume distortions are calculated using the maximum-volume polyhedron for respective CN (7 for a regular pentagonal bipyramid, 4 for a regular tetrahedron) as ideal reference. Sphere radius is expressed in Å, whereas sphere volume and polyhedron volume are expressed in Å^3.

(1) Volume distortion ν = [V(ideal) – V(polyhedron]/V(ideal) to be multiplied by 100 to obtain percentage.

(2) "Volume-based" eccentricity $ECC_v = 1 - [(r_s - \Delta)/r_s]^3$, where r_s is the radius of the circumscribed sphere, and Δ is the distance between the sphere's center ("centroid") and the central atom.

(3) "Volume-based" sphericity $SPH_v = 1 - 3\sigma_r r_s$, where σ_r is a standard deviation of the radius r_s.

Values indicated by a "u" are valid for a refinement with an unsplit (Bi.Pb)3 position; those indicated by "s" describe a refinement with a pair of sites, Bi 3 and Pb 2.

to [010]* (our notation) in the diffraction images of oversubstituted krupkaite and an intergrowth of aikinite "units" in a krupkaite matrix in the corresponding HRTEM images. This does not contradict our results on krupkaite (n_{aik} = 59), which also shows faint streaks parallel to [010]*, interconnecting and surrounding some strong, sharp reflections. Our data suggest that for the crystal from the Felbertal deposit, the formation of randomly scattered strips of aikinite, which presumably are of only finite length (see Pring 1995), proceeds *via* conversion of some of those (010) planes in krupkaite, which contain Bi + tetrahedral vacancies, into occasional (fragments of) planes containing Pb + Cu. It does not proceed *via* insertion of aikinite strips that are one ribbon or an odd number of ribbons thick: such strips would offset the following portion of krupkaite structure by ½*b* and create anti-phase domains, which ought to show up in the structure refinement as partial occupancies of the Cu 1 and Cu 2 sites in different proportions. This phenomenon might account for the 80:20 occupancy ratio for the two Cu sites in the structure refinement of krupkaite by Mumme (1975). It should be noted that during the structure refinement, krupkaite (n_{aik} = 59) was treated as an untwinned crystal, and the Flack parameter, indicated by the SHELXTL program, fluctuated between zero and 0.1, with a standard deviation of 0.03. The pattern of distribution for excess Cu in the structure of oversubstituted gladite, found in this study, precludes its explanation by insertion of krupkaite-like strips in the structure of gladite.

Acknowledgements

This project was supported by the research grants of the Danish Natural Science Research Council and by a grant to D. Topa from the University of Salzburg, Austria. The professional help of Miss Helene Almind and Mrs. Camilla Sarantaris as well as the helpful suggestions of D.J.M. Bevan, A. Pring and R.F. Martin are gratefully acknowledged.

References

Balić-Žunić, T. & Makovicky, E. (1996): Determination of the centroid or "the best centre" of a coordination polyhedron. *Acta Crystallogr.* **B52**, 78-81.

_____, Topa, D. & Makovicky, E. (2002): The crystal structure of emilite, $Cu_{10.7}Pb_{10.7}Bi_{21.3}S_{48}$, the second 45 Å derivative of the bismuthinite–aikinite solid-solution series. *Can. Mineral.* **40**, 239-245.

Borodayev, Y.S., Mozgova, N.N. & Vyalsov, L.N. (1970): The isomorphous series bismuthinite–aikinite. *Vestnik Mosk. Univ.* **1970**(1), 18-33 (in Russ.).

Chen, T.T., Kirchner, E. & Paar, W. (1978): Friedrichite, $Cu_5Pb_5Bi_7S_{18}$, a new member of the aikinite–bismuthinite series. *Can. Mineral.* **16**, 127-130.

Ciobanu, C. & Cook, N.J. (2000): Intergrowths of bismuth sulphosalts from the Ocna de Fier Fe-skarn deposit, Banat, southwest Romania. *Eur. J. Mineral.* **12**, 899-917.

Harris, D.C. & Chen, T.T. (1976): Crystal chemistry and re-examination of nomenclature of sulfosalts in the aikinite–bismuthinite series. *Can. Mineral.* **14**, 194-205.

Horiuchi, H. & Wuensch, B.J. (1976): The ordering scheme for metal atoms in the crystal structure of hammarite, $Cu_2Pb_2Bi_4S_9$. *Can. Mineral.* **14**, 536-539.

_____ & _____ (1977): Lindströmite, $Cu_3Pb_3Bi_7S_{15}$: its space group and ordering scheme for metal atoms in the crystal structure. *Can. Mineral.* **15**, 527-535.

Kohatsu, I. & Wuensch, B.J. (1971): The crystal structure of aikinite, $PbCuBiS_3$. *Acta Crystallogr.* **B27**, 1245-1252.

_____ & _____ (1976): The crystal structure of gladite, $PbCuBi_5S_9$, a superstructure intermediate in the series Bi_2S_3–$PbCuBiS_3$ (bismuthinite–aikinite). *Acta Crystallogr.* **B32**, 2401-2409.

Kupčík, V. & Veselá-Nováková, L. (1970): Zur Kristallstruktur des Bismuthinits, Bi_2S_3. *Tschermaks Mineral. Petrogr. Mitt.* **14**, 55-59.

Makovicky, E. & Balić-Žunić, T. (1998): New measure of distortion for coordination polyhedra. *Acta Crystallogr.* **B54**, 766-773.

_____ & Makovicky, M. (1978): Representation of compositions in the bismuthinite–aikinite series. *Can. Mineral.* **16**, 405-409.

_____, Topa, D. & Balić-Žunić, T. (2001): The crystal structure of paarite, the newly discovered 56 Å derivative of the bismuthinite-aikinite solid-solution series. *Can. Mineral.* **39**, 1377-1382.

Mozgova, N.N., Nenasheva, S.N., Chistyakova, N.I., Mogilevkin, S.B. & Sivtsov, A.V. (1990): Compositional fields of minerals in the bismuthinite–aikinite series. *Neues Jahrb. Mineral., Monatsh.*, 35-45.

Mumme, W.G. (1975): The crystal structure of krupkaite, $CuPbBi_3S_6$, from the Juno mine at Tennant Creek, Northern Territory, Australia. *Am. Mineral.* **60**, 300-308.

_____ & Watts, J.A. (1976): Pekoite, $CuPbBi_{11}S_{18}$, a new member of the bismuthinite–aikinite mineral series: its crystal structure and relationship with naturally- and synthetically-formed members. *Can. Mineral.* **14**, 322-333.

_____, Welin, E. & Wuensch, B.J. (1976): Crystal chemistry and proposed nomenclature for sulfosalts intermediate in the system bismuthinite–aikinite (Bi_2S_3–$CuPbBiS_3$). *Am. Mineral.* **61**, 15-20.

Ohmasa, M. & Nowacki, W. (1970a): Note on the space group and on the structure of aikinite derivatives. *Neues Jahrb. Mineral., Monatsh.*, 158-162.

_____ & _____ (1970b): A redetermination of the crystal structure of aikinite ($BiS_2Cu(IV)Pb(VII)$). *Z. Kristallogr.* **132**, 71-86.

PRING, A. (1989): Structural disorder in aikinite and krupkaite. *Am. Mineral.* **74**, 250-255.

_____ (1995): Annealing of synthetic hammarite, $Cu_2Pb_2Bi_4S_9$, and the nature of cation-ordering processes in the bismuthinite–aikinite series. *Am. Mineral.* **80**, 1166-1173.

SYNEČEK, V. & HYBLER, J. (1974): The crystal structure of krupkaite, $CuPbBi_3S_6$, and of gladite, $CuPbBi_5S_9$, and the classification of superstructures in the bismuthinite–aikinite group. *Neues Jahrb. Mineral., Monatsh.*, 541-560.

THALHAMMER, O.A.R., STUMPFL, E.F. & JAHODA, R. (1989): The Mittersill scheelite deposit, Austria. *Econ. Geol.* **84**, 1153-1171.

TOPA, D., BALIĆ-ŽUNIĆ, T., MAKOVICKY, E. (2000): The crystal structure of $Cu_{1.6}Pb_{1.6}Bi_{6.4}S_{12}$, a new 44.8 Å derivative of the bismuthinite–aikinite solid-solution series. *Can. Mineral.* **38**, 611-616.

_____, MAKOVICKY, E. & PAAR, W. (2002): Composition ranges and exsolution pairs for the members of the bismuthinite–aikinite series from Felbertal, Austria. *Can. Mineral.* **40**, 849-869.

WELIN, E. (1966): Notes on the mineralogy of Sweden. 5. Bismuth-bearing sulphosalts from Gladhammar, a revision. *Arkiv för Mineralogi och Geologi* **4**, 377-386.

ŽÁK, L, SYNEČEK, V. & HYBLER, J. (1975): Krupkaite, $CuPbBi_3S_6$, a new mineral of the bismuthinite–aikinite group. *Neues Jahrb. Mineral., Monatsh.*, 533-541.

Received February 1, 2002, revised manuscript accepted July 11, 2002.